

FUNDAMENTALS & APPLICATIONS

CHEMELECTROCHEM

ANALYSIS & CATALYSIS, BIO & NANO, ENERGY & MORE

Accepted Article

Title: Mediated Catalytic Voltammetry of Holo and Heme-free Human Sulfite Oxidases

Authors: Palraj Kalimuthu, Abdel A Belaidi, Guenter Schwarz, and Paul V. Bernhardt

This manuscript has been accepted after peer review and appears as an Accepted Article online prior to editing, proofing, and formal publication of the final Version of Record (VoR). This work is currently citable by using the Digital Object Identifier (DOI) given below. The VoR will be published online in Early View as soon as possible and may be different to this Accepted Article as a result of editing. Readers should obtain the VoR from the journal website shown below when it is published to ensure accuracy of information. The authors are responsible for the content of this Accepted Article.

To be cited as: *ChemElectroChem* 10.1002/celc.201600685

Link to VoR: <http://dx.doi.org/10.1002/celc.201600685>

WILEY-VCH

www.chemelectrochem.org

A Journal of



Mediated Catalytic Voltammetry of Holo and Heme-free Human Sulfite Oxidases


Palraj Kalimuthu,^a Abdel A. Belaidi,^{b,c} Guenter Schwarz^c and Paul V. Bernhardt^{a,*} 

Herein, we report the electrocatalytic voltammetry of holo and heme-free human sulfite oxidase (HSO) mediated by the synthetic iron complexes 1,2-bis(1,4,7-triaza-1-cyclononyl)ethane iron(III) bromide, ([Fe(dtne)]Br₃·3H₂O), potassium ferricyanide (K₃[Fe(CN)₆]) and ferrocene methanol (FM) at a 5-(4'-pyridinyl)-1,3,4-oxadiazole-2-thiol (Hpyt) modified gold working electrode. Holo HSO contains two electroactive redox cofactors comprising a mostly negatively charged cyt *b*₅ (heme) domain and a Mo cofactor (Moco) domain (the site of sulfite oxidation) where the surface near the active site is positively charged. We anticipated different catalytic voltammetry based on either repulsive or attractive electrostatic interactions between the holo or heme-free enzymes and the positively or negatively charged redox mediators. Both holo and heme-free HSO experimental catalytic voltammetry has been modelled by electrochemical simulation across a range of sweep rates and concentrations of each substrate and both positive and negatively charged electron acceptors ([Fe(dtne)]³⁺, [Fe(CN)₆]³⁻ and FM⁺) which provides new insights into the kinetics of the HSO catalytic mechanism. These mediator complexes have almost the same redox potential (all lying in the range +415 to +430 mV vs NHE) and thus deliver the same driving force for electron transfer with the Mo cofactor. However, differences in the electrostatic affinities between HSO and the mediator have a significant influence on the electrocatalytic response.

^[a] Dr P. Kalimuthu, Prof. P. V. Bernhardt, School of Chemistry and Molecular Biosciences, University of Queensland, Brisbane, 4072, Australia. E-mail: p.bernhardt@uq.edu.au

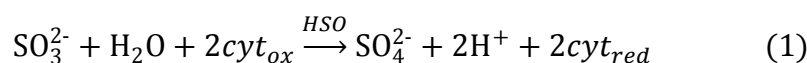
^[b] Dr. A.A. Belaidi, The Florey Institute of Neuroscience and Mental Health, University of Melbourne, Victoria, 3052, Australia

^[c] Prof. G. Schwarz, Institute of Biochemistry, Department of Chemistry and Center for Molecular Medicine, Cologne University, Zùlicher Str. 47, 50674 Kùln, Germany

 Supporting Information for this article is available on the WWW

1. Introduction

Humans sulfite oxidase (HSO) is a homodimeric protein located in the inter-membrane space of mitochondria that oxidises toxic sulfite to sulfate using cytochrome *c* as the oxidant (equation 1). HSO is a homodimeric protein and each monomer (52 kDa) comprises three domains; a *b*-type heme domain (~10 kDa) at the N-terminus which is linked by a flexible polypeptide loop to a larger component (~ 42 kDa) that harbours the Mo cofactor active site and dimerization domains (Figure 1).^[1] Due to the acute toxicity of sulfite, lack of HSO function (usually due to genetic disorders) in neonates leads to severe brain damage and death. HSO activity is necessarily absent in people suffering Mo cofactor (Moco) deficiency as this cofactor is essential for enzyme function. Recent success has been reported in treating Moco deficiency by supplementing patients with cyclic pyranopterin monophosphate (cPMP), a precursor to Moco.^[2]



Sulfite is oxidised to sulfate at the Moco (Mo^{VI}) active site. The reduced (Mo^{IV}) cofactor donates these electrons, one at a time, to the heme cofactor so the heme and Moco must be in proximity for electron transfer and proper catalytic function. The flexible polypeptide loop that connects the heme and Moco domains plays an important role and it has been shown that the relative orientation of the Moco and heme domains is variable. In fact the crystal structure of chicken sulfite oxidase (CSO), which shares 68% sequence identity with HSO, found the heme and Moco domains remote from one another in an inactive conformation (shown in cartoon form in Figure 1, right).^[1a] No crystal structure of holo HSO is available but a crystal structure of the heme domain has been reported^[3] along with a homology model of the Moco domain based on its similarity to CSO.^[1a] This has enabled a model for the ideal orientation of the two domains to be proposed (Figure 1). The heme subunit is predominantly negatively charged and is thought to dock adjacent to the Moco domain near a patch of positively charged surface

amino acid residues (shown in blue in the middle of Figure 1, left). After catalysis the two electrons from sulfite oxidation are transferred, *via* the heme domain, to ferricytochrome *c* as represented in equation 1.^[4]

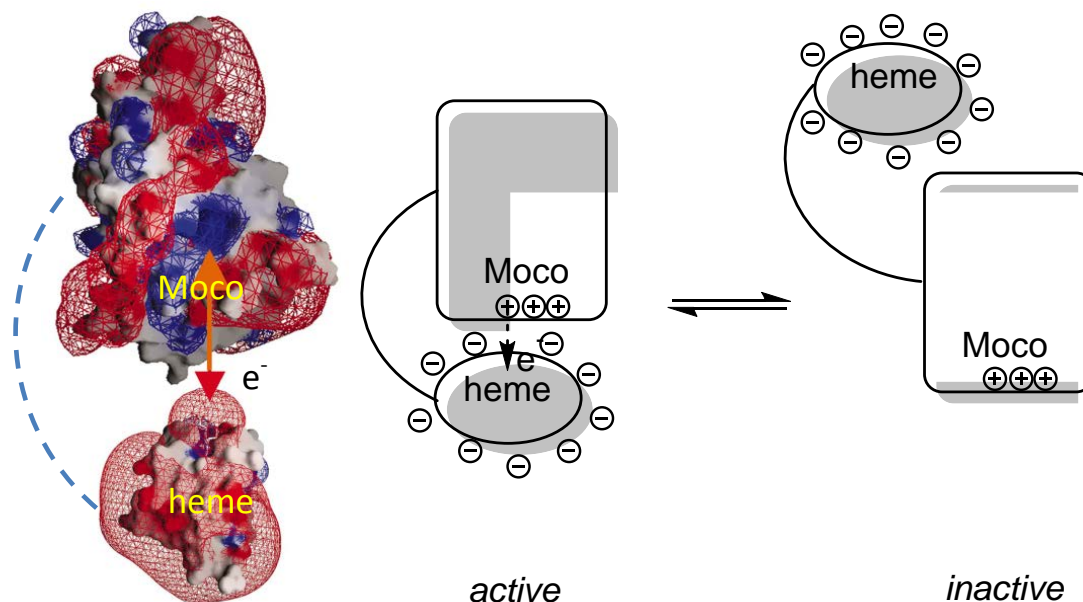


Figure 1. Illustration of the electrostatic surfaces of the Moco and heme domains in holo HSO. (Left) bottom: heme domain from its crystal structure^[3] and top homology model of HSO Moco domain (flexible polypeptide represented by broken line); (right) cartoon representation of HSO conformational flexibility. Adapted from reference 3 with permission of the International Union of Crystallography

The natural electron acceptor ferricytochrome *c* can be replaced by an electrode if SO is immobilized on a suitable functionalized conducting support, which allows a triggering of the catalytic cycle with potentiostatic control. The unmediated voltammetry of vertebrate SOs was successfully demonstrated by several groups on various modified electrodes.^[5] It was found that the heme domain of SO is directly accessible at the electrode surface and acts as a relay for electrical communication between the Moco active site and electrode surface. This unmediated (direct) voltammetry was achieved using a variety of chemically modified electrodes including positively charged functionalized electrodes including $-\text{NH}_3^+$ terminated self-assembled monolayers,^[5b] polyethelene imine entrapped

semiconductor quantum dots^[5e] and gold nanoparticles.^[5f, 5g] It is expected that electrostatic attraction between the predominantly negatively charged heme domain and positively charged functionalized surfaces facilitates direct electron transfer.

The catalytic activity of individual domains of SO (Moco and cyt b_5) has been of interest for a better understanding of biological intramolecular electron transfer which is part of catalysis.^[6] The Mo domain and cyt b_5 domains in vertebrate SO are separable by trypsin cleavage.^[6a] The electrochemistry of the cyt b_5 domain was successful on different modified electrodes but it did not show any catalytic activity toward sulfite oxidation, as expected.^[6b, 7] In contrast, there is no report of direct voltammetry of the Mo domain. The Mo cofactor is buried inside the relatively large domain thus hindering direct electrochemistry. Alternatively, low molecular weight redox active compounds may be used as electron transfer mediators which can undergo homogeneous electron transfer with the enzyme cofactors. The efficiency of mediated electron transfer mainly depends both on the thermodynamic driving force *i.e.* the difference between the formal potentials of the enzyme redox cofactor and the mediator, and the distance between the two redox centres. The Mo domain of HSO may undergo electron transfer with its natural electron acceptor cyt c ^[6d] and also with synthetic electron acceptor osmium complexes.^[6c] However, the overall rate of sulfite oxidation was very slow at the (heme-free) Mo domain of a HSO modified electrode relative to holo HSO. On the other hand, the Mo domain of chicken SO doesn't transfer electrons to its natural electron acceptor cyt c but transfers electrons to the artificial electron acceptor ferricyanide.^[8]

Very recently, we reported the catalytic voltammetry of holo HSO with the positively charged mediators bis(1,4,7-triazacyclononane)iron(III) ($[\text{Fe}(\text{tacn})_2]^{3+}$) and 1,2-bis(1,4,7-triaza-1-cyclononyl)ethane iron(III) ($[\text{Fe}(\text{dtne})]^{3+}$) at a glassy carbon working electrode with HSO entrapped beneath a semi-permeable membrane.^[9] Interestingly, we found that these positively charged mediators accumulated under the membrane in the presence of holo HSO and showed an enhanced redox response compared

with a bare GC electrode. It is presumed that the positively charged mediators were electrostatically attracted to the negatively charged cyt b_5 domain of holo HSO and facilitated electron transfer. To obtain a deeper insight into these electrostatic interactions and also regarding electron transfer mechanisms of HSO with mediators, we have investigated the catalytic voltammetry of holo HSO as well as heme-free HSO with both positively and negatively charged mediators at a chemically modified Au working electrode. The $\text{Mo}^{\text{VI/V}}$ and heme ($\text{Fe}^{\text{III/II}}$) redox potentials of HSO are very close (+41 and +62 mV vs NHE at pH 7.5 respectively).^[10] Thus, we have chosen three high potential mediators (Figure 2) which may act as effective redox partners for both holo and heme-free HSO.

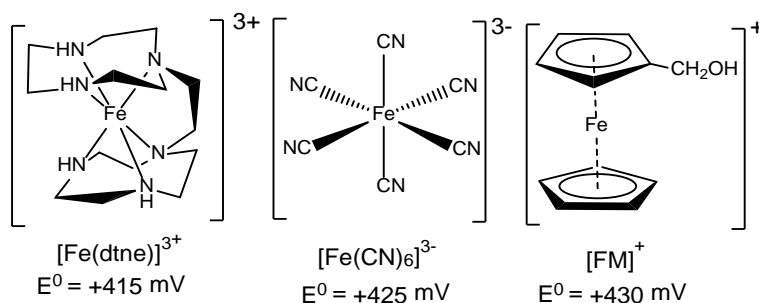


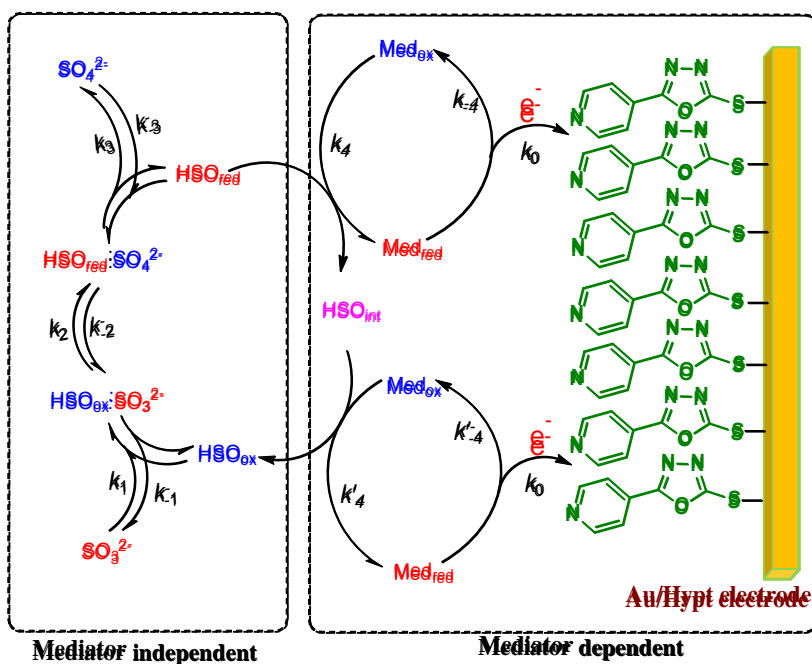
Figure 2. Molecular structures and redox potentials of the mediators used in this study.

As a complement to this work we have carried out the electrochemical simulation of the catalytic voltammetry of both holo and heme-free HSO. Electrochemical simulation was performed to determine the rate and equilibrium constants of the various steps involved in the mediated electrochemical catalysis of holo and heme-free HSO catalysis reaction and also the reaction with their artificial electron partners by modelling the catalytic voltammograms over a range of concentrations of both positively and negatively charged mediators and substrate concentrations. The redox potential of mediators are almost same (in the range +415 to + 430 mV) and so the intrinsic driving force does not play a role and it is possible to gauge the effects of charge on the kinetics of electron transfer in this system.

2. Results and Discussion

Mediated Electrocatalytic Mechanism of HSO

The general electrocatalytic mechanism of HSO is depicted in Scheme 1. The complexes $[\text{Fe}(\text{dtne})]^{3+}$, $[\text{Fe}(\text{CN})_6]^{3-}$ and FM^+ were used as artificial electron transfer partners for HSO. They mimic cytochrome *c* in being one-electron acceptors and must react twice with the sulfite-reduced form of HSO to restore it to its active form. Holo HSO contains two redox active cofactors and two intramolecular electron transfer (IET) processes take place during regeneration of HSO_{ox} by the iron complexes. The first IET step occurs when sulfite-reduced HSO_{red} initially in its $\text{Mo}^{\text{IV}}/\text{Fe}^{\text{III}}$ state transfers one electron from Mo to Fe. The ensuing $\text{Mo}^{\text{V}}/\text{Fe}^{\text{II}}$ species transfers one electron to the mediator (via the heme) producing the transient $\text{Mo}^{\text{V}}/\text{Fe}^{\text{III}}$ state (rate constant k_4), which reverts to the more stable $\text{Mo}^{\text{VI}}/\text{Fe}^{\text{II}}$ state through a second IET step. The second electron is transferred to another mediator molecule (rate constant k'_4) restoring the fully oxidized HSO_{ox} ($\text{Mo}^{\text{VI}}/\text{Fe}^{\text{III}}$) state of the enzyme.



Scheme 1. Mediated Electrochemically Driven Catalysis of HSO.

On the other hand, heme-free HSO contains only the Moco domain and must directly transfer electrons to the mediator without any IET. The kinetics of IET in SO enzymes has been extensively studied^[10-11] and this reaction is rapid by comparison with the bimolecular reactions shown in Scheme 1 so we have not included IET steps in our kinetic model. The substrate (sulfite) and mediator ($[\text{Fe}(\text{dtne})]^{3+}$) or $[\text{Fe}(\text{CN})_6]^{3-}$ or FM^+) are under diffusion control in solution whereas holo HSO or heme-free HSO are confined to the electrode surface under the dialysis membrane. Mass transport limitations due to passage across the dialysis membrane of mediators and substrates during the catalytic reaction are accounted for by slightly attenuated diffusion coefficients. It is important to note that this is a ternary system and all three components (HSO, mediator and sulfite) must be present for catalysis.

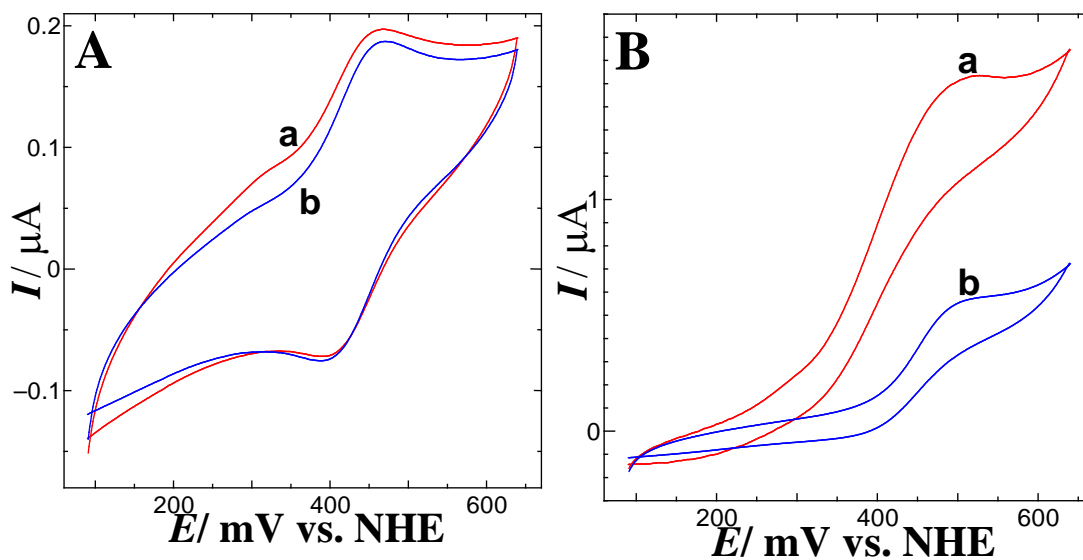


Figure 3. CVs obtained for 100 μM FM (A) in the absence and (B) in the presence of 800 μM sulfite at (a) a Au/Hpyt/holo HSO electrode and (b) a Au/Hpyt/heme free HSO electrode in 50 mM Tris buffer (pH 8.0) at a scan rate of 5 mV s^{-1} .

Catalytic Voltammetry of HSOs with Positively Charged Mediators

The role of electrostatic interactions in the catalytic activity of holo and heme-free HSO was investigated with the positively charged synthetic mediators FM^+ and $[\text{Fe}(\text{dtne})]^{3+}$ and one negatively

charged mediator $[\text{Fe}(\text{CN})_6]^{3-}$. Figure 3 illustrates the catalytic voltammetry of holo and heme-free HSO at each Au/Hpyt electrode in the presence of the mono-positively charged electron acceptor FM^+ . In the absence of sulfite (Figure 3A) both the holo and heme-free HSO modified Au/Hpyt electrodes show the $\text{FM}^{+/0}$ redox response at +430 mV with a peak-to-peak separation of 60 mV for 100 μM FM, which is in agreement with Nernstian behaviour for a one-electron transfer process. However there is a subtle difference in the voltammetry for holo HSO (Figure 3A, curve a) and heme-free HSO (Figure 3A, curve b). Firstly, the oxidation current response of FM is slightly higher at the holo HSO modified electrode compared to the heme-free HSO modified electrode (Figure 3A, curve b). Secondly, the holo HSO modified electrode shows a small pre-wave shoulder around +320 mV in addition to the expected $\text{FM}^{+/0}$ couple centred at +460 mV. In contrast, the pre-wave is absent at the heme-free HSO modified electrode. The enhanced FM redox response in addition to the pre-wave is caused by association between FM^+ and anionic surface amino acid residues of the heme domain of holo HSO.^[1a, 12] In contrast, the heme-free HSO contains only the Moco domain which bears more positively charged surface amino acid residues, particularly near its active site, that assist in attracting the negatively charged substrate (SO_3^{2-}) but repel positively charged the electron acceptors (Figure 3) and consequently decreases the catalytic current.

The catalytic activity of holo and heme-free HSO was examined by adding 800 μM sulfite to the electrochemical cell containing 100 μM FM. As shown in Figure 3B the observed catalytic response is entirely different at the holo and heme-free HSO electrodes even though the concentration of enzymes (3 μL of 50 μM), mediators and sulfite are the same. A well-defined, almost sigmoidal catalytic oxidation waveform was observed with no cathodic wave at both HSOs electrodes. However, the holo HSO electrode (Figure 3B, curve a) shows a nearly 3-fold higher catalytic current for sulfite oxidation compared to the heme-free HSO electrode (Figure 3B, curve b) and also the catalytic potential is *ca.* 100

mV lower for holo HSO than heme-free HSO. In a control experiment, in the absence of HSO but in the presence of 100 μM FM non-specific sulfite oxidation occurs at potentials above +550 mV at the Au/Hpyt electrode (Supporting information, Figure S1), so all scans were reversed before this potential was reached. The observed sigmoidal voltammetric waveform is characteristic of a catalytic homogeneous reaction coupled to heterogeneous electron transfer (EC_{cat} mechanism)^[13] where sulfite is oxidized enzymatically yielding the two electron reduced form of the enzyme, which is oxidized again by electro-generated FM^+ .

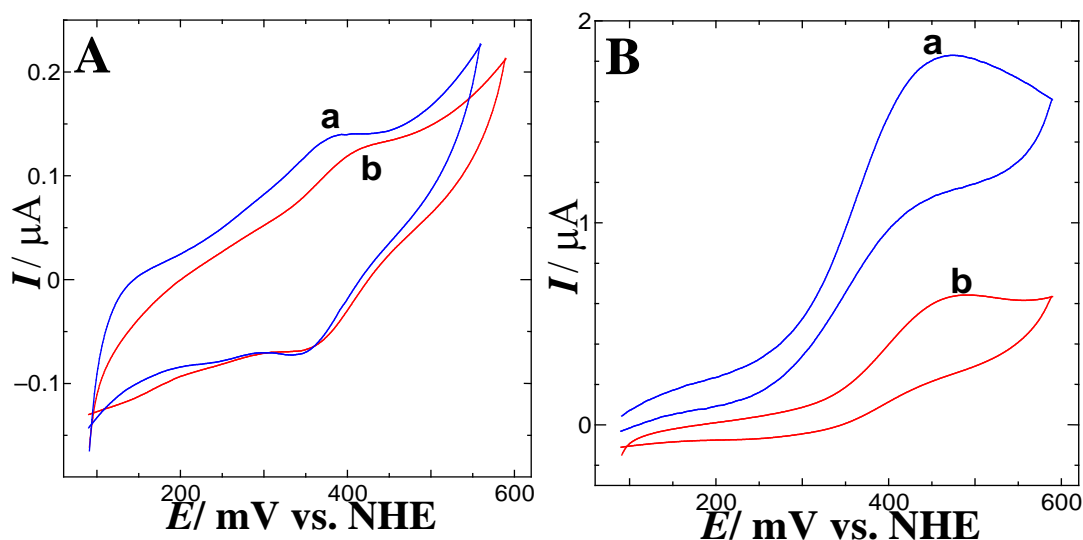


Figure 4. CVs obtained for $50 \mu\text{M}$ $[\text{Fe}(\text{dtne})]^{3+}$ (A) in the absence and (B) presence of 2.4 mM sulfite at (a) a Au/Hpyt/holo HSO and (b) Au/Hpyt/heme-free HSO electrode in 50 mM Tris buffer (pH 8.0) at a scan rate of 5 mV s^{-1} .

To confirm that electrostatic interactions between the mediator and enzyme were responsible for the differences in catalytic activity, we investigated the voltammetry of both holo and heme-free HSO with the tri-positively charged mediator $[\text{Fe}(\text{dtne})]^{3+}$. Figure 4A illustrates the redox response of $[\text{Fe}(\text{dtne})]^{3+}$ at the holo and heme-free HSO modified Au/Hpyt electrodes. In the very first cycle, a

pronounced oxidation peak at +365 mV with a weak reduction wave at +320 mV was observed for 50 μM $[\text{Fe}(\text{dtne})]^{3+}$ at the holo HSO modified electrode (Supporting Information, Figure S2A). Again the higher mediator oxidation current in the first cycle is due to accumulation of mediator molecules at the vicinity of the electrode by electrostatic attraction to HSO trapped under the membrane near the electrode surface. In the second cycle, the anodic peak diminished and from the third cycle onwards both oxidation and reduction waves became approximately equal in magnitude eventually centred at +368 mV with a peak to peak separation of 35 mV. The small peak-to peak separation and the cathodically shifted $\text{Fe}^{\text{III/II}}$ redox couple are attributable to a strong association between the $[\text{Fe}(\text{dtne})]^{3+}$ and HSO localized near the negatively charged heme domain leading to a response that is more consistent with a surface immobilized redox reaction. These results are consistent with our recent report for the electrochemistry positively charged complexes with holo HSO at a glassy carbon electrode.^[9]

The redox response of $[\text{Fe}(\text{dtne})]^{3+}$ was also examined at the heme-free HSO electrode. Interestingly, the redox response of the mediator is virtually unchanged over 20 repeat cycles indicating no significant interaction between heme-free HSO and the positively charged mediator (Supporting information, Figure S2B). The $[\text{Fe}(\text{dtne})]^{3+}$ redox peak is positioned at +382 mV with a peak to peak separation of 56 mV, which is normal for a diffusion controlled single electron reaction.

Upon introduction of 2.4 mM sulfite to the electrochemical cell a pronounced catalytic response was observed at both the holo and heme-free HSO modified electrodes (Figure 4B). However, the catalytic current at the holo HSO electrode (curve a) is nearly 3-fold greater than at the heme-free HSO modified electrode (curve b) and again the catalytic potential is lowered by ca. 70 mV for the holo HSO system. This reinforces the point that the negatively charged heme domain of holo HSO is more strongly attracted to the positively charged $[\text{Fe}(\text{dtne})]^{3+}$ mediator and this enhances the catalytic response by

facilitating effective electron transfer and lowering the catalytic potential. A similar observation reported for the catalytic voltammetry of holo and heme-free HSOs with a positively charged osmium complex at a carbon electrode found that the catalytic response of heme-free HSO was only 30 % relative to that from holo HSO.^[6c]

Catalytic Voltammetry of HSOs with a Negatively Charged Mediator

To further examine the electrostatic interactions between holo and heme-free HSO and the mediator, we employed the tri-negatively charged mediator $[\text{Fe}(\text{CN})_6]^{3-}$ under the same experimental conditions as before and the results are displayed in Figure 5. The holo HSO electrode shows a redox peak at +408 mV with a peak to peak separation of 135 mV for 0.5 mM $[\text{Fe}(\text{CN})_6]^{3-}$ (Figure 5A, curve a).

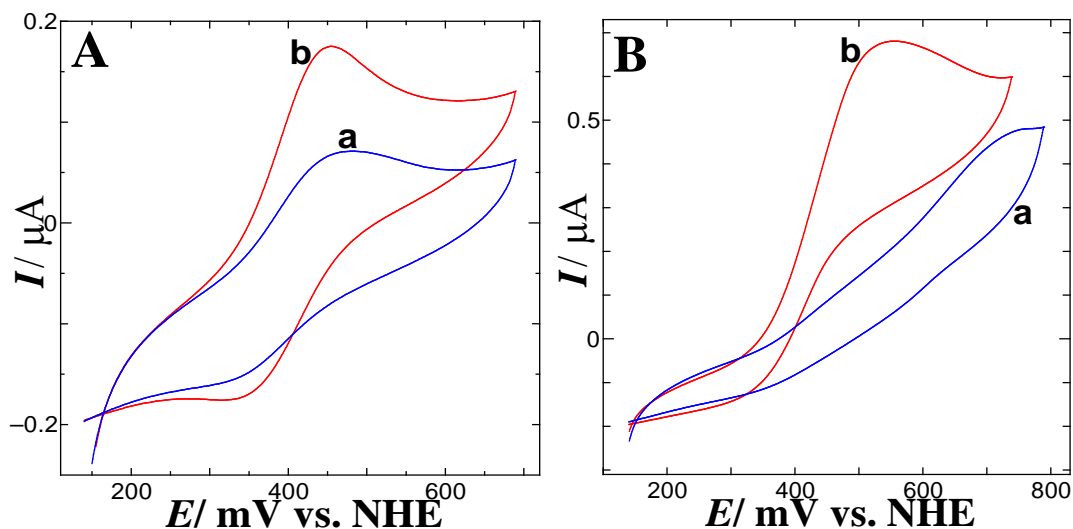


Figure 5. CVs obtained for 500 μM $\text{K}_3\text{Fe}(\text{CN})_6$ in absence (A) and presence (B) of 800 μM sulfite at (a) Au/Hpyt/holo HSO and (b) Au/Hpyt/heme-free HSO electrode in 50 mM Tris buffer (pH 8.0) at a scan rate of 5 mV s^{-1} .

In the absence of sulfite, no significant change in this voltammogram was observed for 20 continuous sweeps at the holo HSO electrode (Supporting information, Figure S2C). In contrast, a

pronounced anodic peak was observed for 0.5 mM of $[\text{Fe}(\text{CN})_6]^{3-}$ at the heme-free HSO electrode in the first cycle (Figure 5A, curve b and Supporting information, Figure S2D). It appears that accumulation of negatively charged ferricyanide under the membrane is favoured by the more positively charged Mo domain of heme-free HSO; the complement of our observations of attraction between holo HSO with $[\text{Fe}(\text{dtne})]^{3+}$. In subsequent cycles (Supporting information, Figure S2D) the wave becomes symmetrical centred at +400 mV with a peak to peak separation of 100 mV. Further, it was noted that the $[\text{Fe}(\text{CN})_6]^{3-}$ redox couple at the heme-free HSO electrode is about 50 mV lower than the holo HSO electrode and also the peak current is notably higher for the heme-free HSO electrode (curve b) than the holo HSO electrode (curve a).

At the holo HSO electrode, upon introduction of 800 μM sulfite to the electrochemical cell in the presence of 500 μM $[\text{Fe}(\text{CN})_6]^{3-}$, the anodic current increased somewhat but the waveform was not entirely consistent with an electrochemically driven catalytic reaction (Figure 5B, curve a). Instead the increase in current at high potential can be attributed partly to non-specific sulfite oxidation ($> +550$ mV). However, at the heme-free HSO electrode, the reversible $[\text{Fe}(\text{CN})_6]^{3-/4-}$ couple at +400 mV is transformed into an amplified, sigmoidal waveform consistent with an enzyme-catalysed electrochemical reaction (Figure 5B, curve b). These results again confirm that electrostatic interactions between the enzyme and mediator play significant roles in electrocatalytic activity.

HSO-Sulfite Reaction

The sulfite-dependence of the electrocatalytic HSO reaction was examined with both positively and negatively charged mediators. Figure 6 shows the effect of increasing concentration of sulfite in the presence of 100 μM FM at holo (Figure 6A) and heme-free HSO (Figure 6B) electrodes. A reversible, diffusion controlled $\text{FM}^{+/0}$ response at +430 mV along with a prewave at +320 mV is seen for 100 μM FM at the holo HSO electrode (Figure 6A, curve a and also Figure 3A, curve a). As mentioned already, the

prewave corresponds to FM^+ molecules that are electrostatically attracted to holo HSO near the electrode surface. In other mediated electrochemical studies of Mo enzyme we have observed similar pre-wave voltammetric responses.^[9, 14]

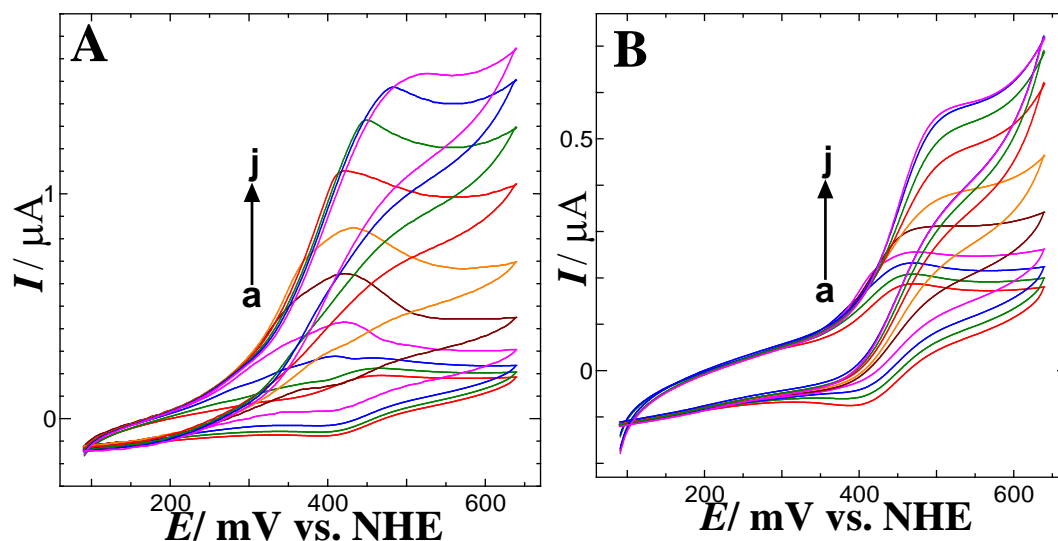


Figure 6. CVs obtained for the increasing concentration of sulfite (a) 0, (b) 25, (c) 50, (d) 100, (e) 200, (f) 400, (g) 800, (h) 1600, (i) 2400 and (j) 3200 μM in the presence of 100 μM FM at (A) Au/Hpyt/holo HSO and (B) Au/Hpyt/heme-free HSO electrode in 50 mM Tris buffer at a scan rate of 5 mV s^{-1} .

The same experiment was repeated at the heme-free HSO electrode and the results appear in Figure 6B. The heme HSO electrode shows no $\text{FM}^{+/0}$ prewave in the absence or presence of sulfite. Instead, the symmetrical, diffusion controlled $\text{FM}^{+/0}$ wave at +420 mV transforms into a sigmoidal steady state waveform with increasing sulfite concentration. We also examined the sulfite concentration dependence of the voltammetry in the presence of $[\text{Fe}(\text{dtne})]^{3+}$ at both the holo and heme-free HSO electrodes and very similar behaviour was seen (Supporting Information Figure S3). Favourable electrostatic interactions between the enzyme and mediator can stabilise the active ferric oxidation state of the mediator significantly leading to a much lower overpotential for catalysis. This is always a

desirable feature as high overpotentials may lead to indiscriminant redox reactions with other molecules in the solution, including direct oxidation of the substrate at the electrode in this case.

For both the holo and heme-free HSO enzymes, the catalytic sulfite oxidation current increased linearly up to approximately 800 μM sulfite before reaching saturation around 3.5 mM. Apparent Michaelis constants ($K_{M,\text{sulfite}}$) of 747 μM and 676 μM were obtained from the Michaelis-Menten plot (current taken at +480 mV) for holo HSO and heme-free HSO electrodes, respectively (Supporting Information, Figure S4). The observed K_m value is almost same at holo and heme-free HSO electrodes and it is consistent with a recent report on electrochemistry of HSO with the polymeric positively charged mediator poly(vinylpyridine)-[osmium-(N,N'-methyl-2,2'-biimidazole) $_3$] $^{3+/2+}$,^[6c] which found an apparent K_M value of 500 and 450 μM for heme-free and Holo HSO, respectively. Conversely, the observed K_M value is very high compared to the value reported from solution assay ($K_m = 9 \mu\text{M}$) for holo HSO with its physiological electron acceptor cytochrome *c*.^[11b] This is due to the mass transport limitations presented by the membrane, which results in the linear response of the electrode to sulfite being increased by an order of magnitude. We have observed similar observations in other Mo enzyme systems.^[14a, 15]

Further, we have examined the enzyme and substrate interaction by increasing concentration of sulfite in the presence of tri-negatively charged $[\text{Fe}(\text{CN})_6]^{3-}$ and results are illustrated in Figure 7. The holo HSO electrode (Figure 7A) shows a quasi-reversible redox response at +400 mV with a peak to peak separation of 135 mV for 0.5 mM $[\text{Fe}(\text{CN})_6]^{3-}$ and this wave both grows in magnitude and shifts to higher potential with increasing sulfite concentration.

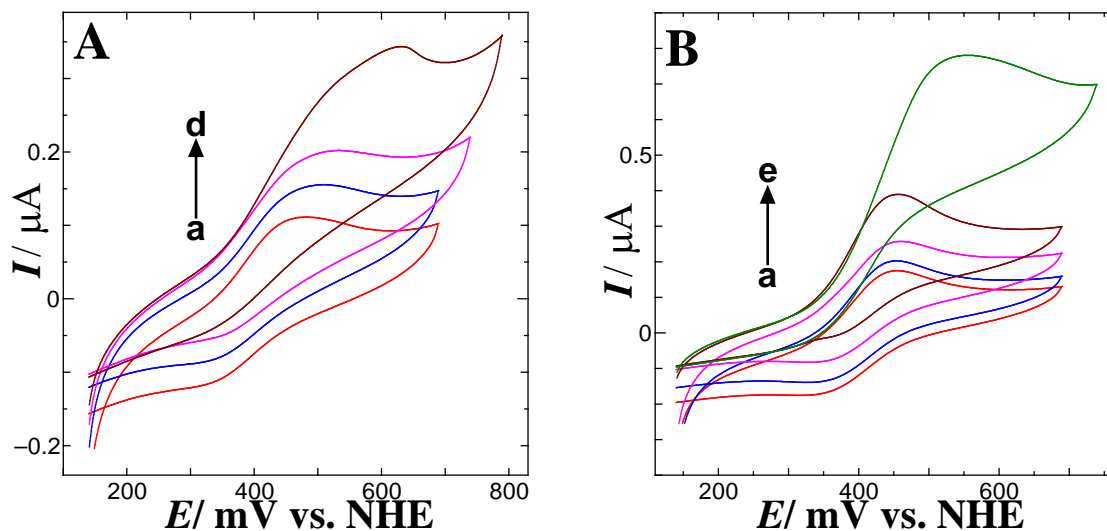


Figure 7. CVs obtained for increasing sulfite concentrations of (a) 0, (b) 100, (c) 200, (d) 400 and (e) 800 μM in the presence of 500 μM $[\text{Fe}(\text{CN})_6]^{3-}$ at (A) a Au/Hpyt/holo HSO and (B) a Au/Hpyt/heme-free HSO electrode in 50 mM Tris buffer at a scan rate of 5 mV s^{-1} .

The heme-free HSO electrode shows a quasi-reversible $[\text{Fe}(\text{CN})_6]^{3-/4-}$ redox response at +400 mV with a peak to peak separation of 100 mV. The catalytic current increases with sulfite concentration but the anodic shift in this catalytic wave is much smaller than seen in the holo HSO voltammetry. Overall, the heme-free HSO electrode shows a higher electrocatalytic current and smaller overpotential with negatively charged $[\text{Fe}(\text{CN})_6]^{3-}$ compared to the holo HSO electrode.

HSO-Mediator Reaction

Figure 8A displays the FM concentration dependence of the catalytic voltammetry in the presence of 2 mM sulfite at a holo HSO electrode. No catalytic activity was seen in the absence of FM at Au/Hpyt/HSO electrode for 2 mM sulfite (Figure 8A, curve a) as direct electrochemistry is not possible under these conditions. However, a sigmoidal voltammogram evolves as FM is introduced to the electrochemical cell, which is indicative of an electrochemical steady state; the forward and backward

sweeps are essentially the same (Figure 8A, curves b-e). However, at high concentration of FM (45 μM , Figure 8A, curve f), the voltammogram becomes peak-shaped. This is due to a large excess of FM^+ being produced at the electrode, which overwhelms the limited amount of HSO_{red} formed during the sulfite oxidation step. Figure 8B displays the similar experiments but at a heme-free HSO modified electrode. Only sigmoidal waves are observed up to 45 μM FM. In both cases the sloping baselines at high potential (> +550 mV) are due to non-specific sulfite oxidation at the electrode.

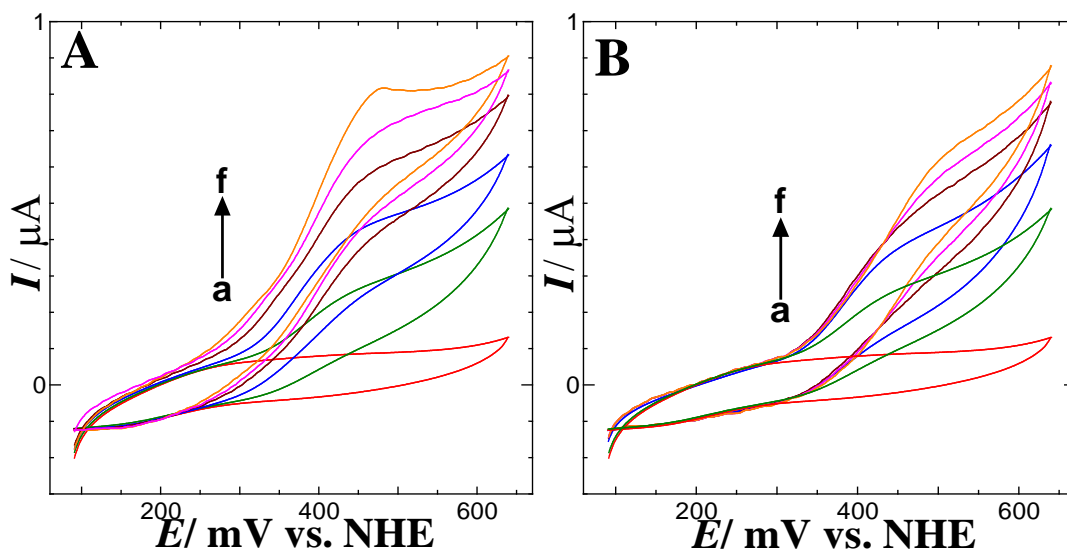


Figure 8. CVs obtained for increasing concentration of FM (a) 0, (b) 5, (c) 15, (d) 25, (e) 35 and (f) 45 μM in the presence of 2.0 mM sulfite at (A) Au/Hpyt/holo HSO and (B) Au/Hpyt/heme-free HSO electrodes in 50 mM Tris buffer at a scan rate of 5 mV s^{-1} .

Table 1. Kinetic parameters (defined in Scheme 1) from electrochemical simulation.

E° mV vs NHE	$[\text{Fe}(\text{dtne})]^{3+}$ 415 mV		$[\text{Fe}(\text{CN})_6]^{3-}$ 425 mV		FM^+ 430 mV	
	holo	Heme-free	holo	Heme-free	holo	Heme-free
k_1 ($\text{M}^{-1} \text{s}^{-1}$)	1.0×10^6	5.0×10^5	1.0×10^6	5.0×10^5	1.0×10^6	5.0×10^5
k_{-1} (s^{-1})	20	10	20	10	20	10
k_2 (s^{-1})	0.8	0.5	0.8	0.5	0.8	0.5
k_{-2} (s^{-1})	0.1	0.1	0.1	0.1	0.1	0.1
k_3 (s^{-1})	1	0.5	1	0.5	1	0.5
k_{-3} ($\text{M}^{-1} \text{s}^{-1}$)	0.1	0.1	0.1	0.1	0.1	0.1
k_4 ($\text{M}^{-1} \text{s}^{-1}$) ^a	2.0×10^6	1.0×10^4	1.0×10^4	1.0×10^5	5.0×10^6	2.0×10^5
k_{-4} ($\text{M}^{-1} \text{s}^{-1}$) ^b	2	5	1	20	2	1
$K_{\text{M},\text{Sulfite}}$ (μM) ^c	21	41	21	41	21	41

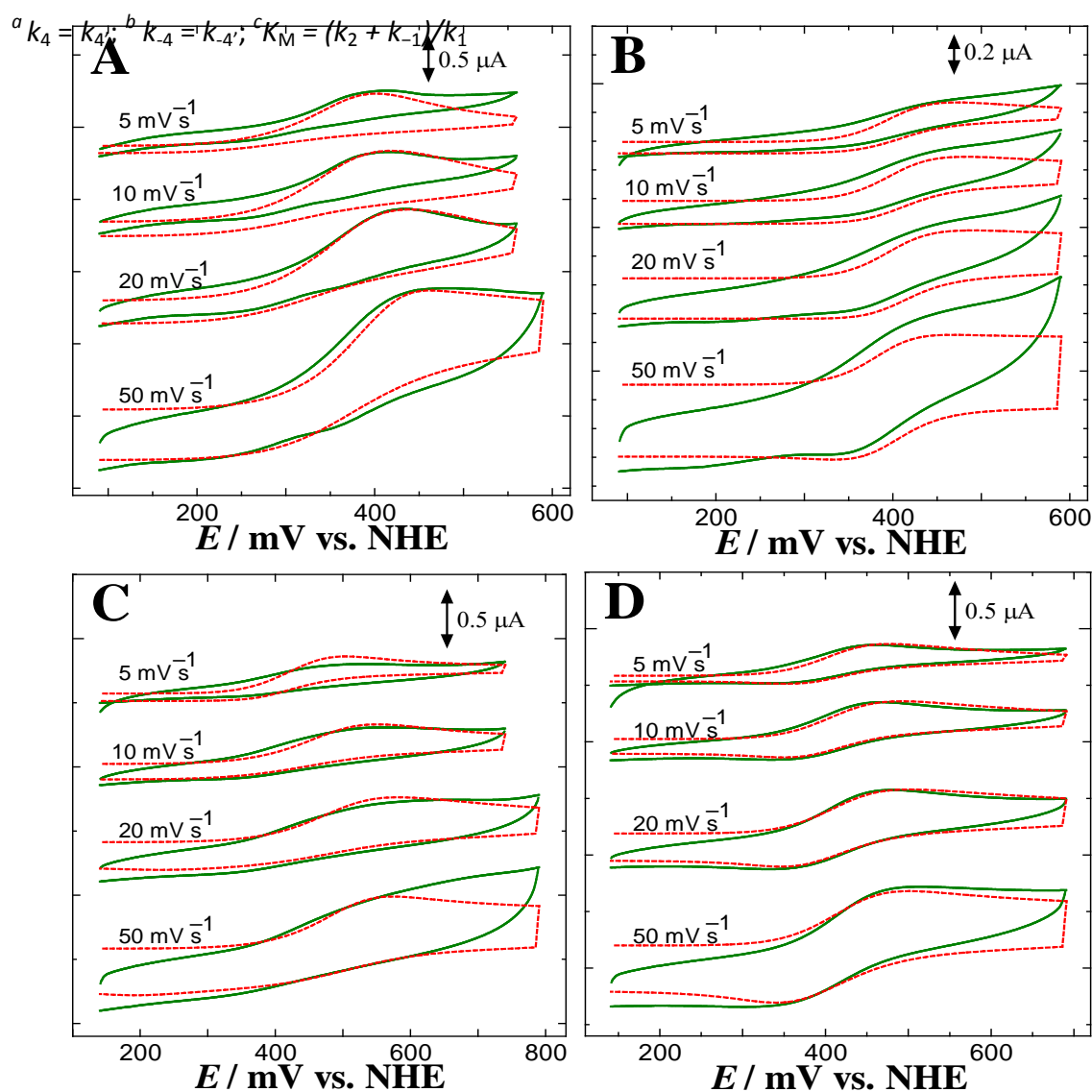


Figure 9. Experimental (solid lines) and simulated (broken lines) sweep rate dependent CVs obtained for 800 μM sulfite in the presence of 50 μM $[\text{Fe}(\text{dtne})]^{3+}$ at (A) Au/Hpyt/olo HSO and (B) Au/Hpyt/heme-

free HSO electrodes. CVs obtained for 200 μM sulfite in the presence of 500 μM $[\text{Fe}(\text{CN})_6]^{3-}$ at (C) Au/Hpyt/holo HSO and (D) Au/Hpyt/heme-free HSO electrodes in 50 mM Tris buffer solution (pH 8).

Electrochemical Simulation

In recent years, we have employed digital simulation for a quantitative understanding of the mechanism of mediated enzyme electrochemical reactions.^[14, 16] The objective of simulation is to obtain values for the rate constants of the homogeneous reactions defined in Scheme 1 that reproduce all voltammetric features over a range of sweep rates, substrate and mediators concentrations. Very recently, we simulated the mediated voltammetry of holo HSO with two positively charged mediators at a glassy carbon electrode.^[9] In that case, the mediators had the same overall charge and very similar structures but significantly different redox potentials. In the present study, the redox potentials are essentially constant while the main changes are in the charge of the mediator and also we have both holo HSO and also heme-free HSO which have shown preferences for oppositely charged electron partners.

The voltammetric sweep rate is a significant variable to elucidate the kinetics of electrochemical processes coupled with chemical reactions as the timescale of the experiment changes thus enabling or disabling coupled chemical reactions at slow or fast sweep rates, respectively. The DigiSim program enables a single set of kinetic parameters (Scheme 1) to be optimized to CVs measured across a range of sweep rates for the same set of enzyme, mediator and substrate concentrations. When the concentrations of mediator and sulfite are varied then ideally the same kinetic parameters reproduce CVs measured under those situations as well. Figure 9 shows the sweep rate dependent experimental and simulated CVs for 800 μM sulfite and 50 μM $[\text{Fe}(\text{dtne})]^{3+}$ (Figure 9A (holo HSO) and Figure 9B (heme-free HSO)) and 200 μM sulfite with 500 μM $[\text{Fe}(\text{CN})_6]^{3+}$ (Figures 9C (holo HSO) and 9D (heme-free HSO)). All other sweep rate dependent voltammograms recorded as a function of various mediator and

substrate concentrations are given in the Supporting Information (Figure S5-S18). The irreversible transient CV at slow sweep rate (5 mV s^{-1}) becomes reversible at higher sweep rate (50 mV s^{-1}) as electrochemical oxidation and reduction of the mediator is too rapid and the homogeneous HSO-mediator reaction becomes uncoupled from heterogeneous electron transfer. These features are well reproduced in the simulation for both positively and negatively charged mediators. Note that the high potential 'tailing' current is due to non-specific sulfite oxidation and this is not part of the model.

The substrate binding rate constant (k_1) is well defined by simulation. Decreasing k_1 by one order at higher concentration of substrate has a major influence on the quality of fit. However, at lower sulfite concentration the k_1 value does not affect the quality of the fit as substrate diffusion (not substrate binding) is rate limiting. The k_2 value (turnover number) defines the overall maximum activity and is accurately quantified by the simulation. However, embedded in this value is the enzyme concentration under the membrane and this is undefined given the uncertainty in the volume of solution trapped under the membrane. The product dissociation rate k_3 value also has a significant influence on the CV if allowed to deviate from its optimal value. Finally, the k_4 values (HSO-mediator outer sphere electron transfer rate) are accurately quantified as the simulation is very sensitive to changes in this value.

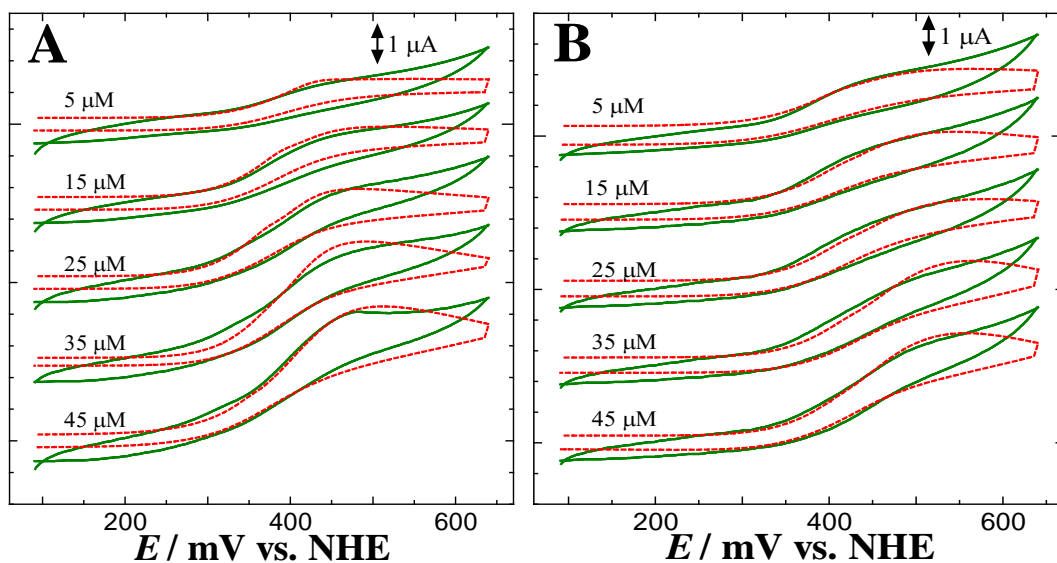


Figure 10. Experimental (solid lines) and simulated (broken lines) CVs obtained for varying FM concentration in the presence of 2 mM of sulfite at (A) Au/Hpyt/holo HSO and (B) Au/Hpyt/heme-free HSO in 50 mM Tris buffer solution (pH 8) at a sweep rate of 5 mV s^{-1} .

Figure 10 shows the CVs as a function of increasing FM concentration (5 – 45 μM) in the presence of 2 mM sulfite at a sweep rate of 5 mV s^{-1} . A classical sigmoidal wave is observed at low FM concentration (5 μM) at the holo HSO modified electrodes (Figure 10A) and this waveform becomes progressively more peak shaped (transient) as the concentration of mediator rises (to 45 μM) as the oxidized mediator overwhelms the amount of holo HSO_{red} present and the electrochemical steady state breaks down. Similar to the holo HSO electrode, a classical sigmoidal wave is observed at low FM concentration (5 μM) at the heme-free HSO modified electrode (Figure 10B). As the FM concentration increases, the catalytic current also increases but shifts anodically and these features are well reproduced in the simulation.

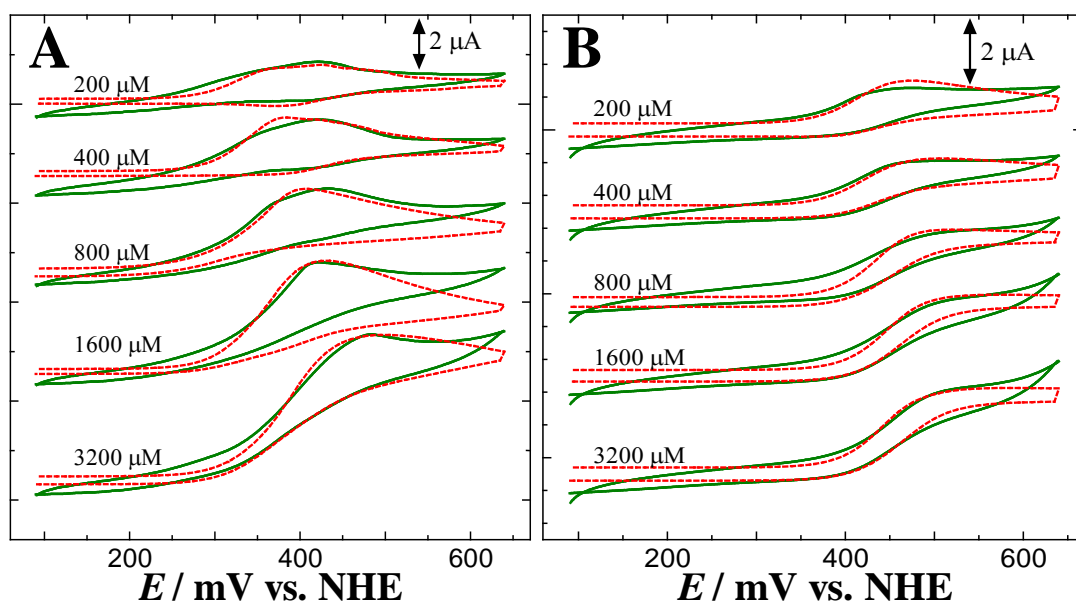


Figure 11. Experimental (solid lines) and simulated (broken lines) CVs obtained for varying sulfite concentration in the presence of (A) 100 μM of FM at (A) Au/Hpyt/holo HSO and (B) Au/Hpyt/heme-free HSO in 50 mM Tris buffer solution (pH 8) at a sweep rate of 5 mV s^{-1} .

The same set of kinetic parameters also reproduced CVs measured at various sulfite concentrations. Figure 11 displays the anodic current response of the Au/Hpyt/holo HSO (Figure 11A) and Au/Hpyt/heme-free HSO (Figure 11B) electrodes as a function of sulfite concentration (200 μM to 3.2 mM) in the presence of 100 μM FM. The different features of voltammograms are noted. At the Au/Hpyt/holo HSO electrode, a reversible voltammogram with a prewave is seen at low sulfite concentrations (200 μM). The prewave features are covered in Figure 6A (*vide supra*) and the reversible transient form of voltammogram is attributed to the excess amount of oxidized mediator on electrode surface. The wave becomes firstly asymmetric as the sulfite concentration rises to 1600 μM where catalysis becomes significant and tailing is due to sulfite depletion. Finally as the enzyme is saturated with sulfite at 3.2 mM the expected steady state sigmoidal waveform is approached. On the other hand, the heme-free HSO electrode shows a reversible transient wave at 200 μM sulfite without any prewave and this wave becomes sigmoidal at 800 μM sulfite.

Analysis of Kinetics Parameters

The rate and equilibrium constants defined in Scheme 1 that reproduced all our experimental voltammetry carried out at different sweep rates, various concentrations of sulfite and mediators are shown in Table 1. One of main objectives of this study to compare the rate and equilibrium constants obtained for holo and heme-free HSO with both positively and negatively charged mediators. The parameters k_1 - k_3 (and k_{-1} - k_{-3}) must be mediator-independent as they only involve homogeneous reactions between the enzyme and sulfite (or product sulfate). However, the heme-free HSO electrode shows a different set of k_1 - k_3 values compared to the holo HSO electrode. The accurate determination of multiple parameters is problematic in that some parameters will have no effect on the CV depending on the concentrations of the reactants. The sulfite binding rate constant determined for holo HSO ($k_1 = 1 \times 10^6 \text{ M}^{-1}\text{s}^{-1}$) in the present study is consistent with our previous report for holo HSO with $[\text{Fe}(\text{dtne})]^{3+}$ at GC electrode.^[9] However, the heme-free HSO shows a slightly lower value ($k_1 = 5 \times 10^5 \text{ M}^{-1}\text{s}^{-1}$).

The turnover number (k_2) obtained in the simulations (0.8 s^{-1} for holo HSO and 0.5 s^{-1} for heme-free HSO) is significantly lower than the experimental value reported by solution assays for wild type HSO with its natural electron acceptor cytochrome *c* in pH 8 (27 s^{-1}).^[11b] Further, the observed value for holo HSO in the present study (0.8 s^{-1}) is lower than we found at an glassy carbon electrode (25 s^{-1}). However, this value is consistent with the electrochemical study of HSO (0.85 s^{-1}) on a mixed self-assembled monolayer modified Ag electrode in 100 mM Tris buffer solution.^[6b] It was found that HSO activity varied towards several factors including pH, ionic strength, composition of the buffer solution and also electrode modification conditions. Only 20 % of HSO was active in an immobilized condition.^[5a, 6b]

The redox potential of the mediators used in the present study are essentially the same (+415 - +430 mV) so variations in k_4 (outer sphere rate constant for mediator – HSO reaction) cannot be

attributed to changes in the driving force, unlike our previous report carried out with mediators of different redox potential.^[9] The observed k_4 value ($2.0 \times 10^6 \text{ M}^{-1} \text{ s}^{-1}$) for holo HSO in reaction with $[\text{Fe}(\text{dtne})]^{3+}$ is consistent with the value obtained for holo HSO on a GC electrode.^[9] However, heme-free HSO shows a two orders of magnitude lower value with $[\text{Fe}(\text{dtne})]^{3+}$ ($k_4 = 1.0 \times 10^4 \text{ M}^{-1} \text{ s}^{-1}$). The same trend is seen with FM^+ as the electron acceptor although the differences in reactivity with holo HSO ($k_4 = 5.0 \times 10^6 \text{ M}^{-1} \text{ s}^{-1}$) and heme-free HSO ($k_4 = 2.0 \times 10^5 \text{ M}^{-1} \text{ s}^{-1}$) are smaller. This smaller discrimination may be attributed to the lower charge of the ferrocenium cation compared with the tripositively charged $[\text{Fe}(\text{dtne})]^{3+}$ complex. Qualitatively similar observations were reported for HSO with its positively charged natural electron acceptor cytochrome *c* on a mixed monolayer modified gold electrode. The second order rate constants for the cytochrome *c* – HSO reaction were reported to be $4.47 \times 10^6 \text{ M}^{-1} \text{ s}^{-1}$ and $1.9 \times 10^5 \text{ M}^{-1} \text{ s}^{-1}$ for holo and heme-free HSO electrodes, respectively.^[6d] Further, we have determined k_4 for the negatively charged mediator $[\text{Fe}(\text{CN})_6]^{3-}$. Holo HSO shows a two order of magnitude lower value in reaction with $[\text{Fe}(\text{CN})_6]^{3-}$ ($k_4 = 1.0 \times 10^4 \text{ M}^{-1} \text{ s}^{-1}$) compared to the positively charged $[\text{Fe}(\text{dtne})]^{3+}$ while ferricyanide is more compatible with heme-free HSO ($k_4 = 1.0 \times 10^5 \text{ M}^{-1} \text{ s}^{-1}$).

$$\log_{10} k_{et} = 13 - 0.6(r - 3.6) - 3.1 \frac{(\Delta G^\circ + \lambda)^2}{\lambda} \quad (2)$$

The rates of outer sphere electron transfer should follow the predictions of Marcus theory and are primarily sensitive to the driving force ΔG° and reorganisational energy λ for redox reactions of small molecules. However, when electron transfer occurs over long distances, such as with redox active proteins, the separation between the two redox partners (r) becomes more important as shown by equation 2.^[17] In the present study, differences in the outer sphere electron transfer rate constants as a function of mediator (Figure 2) cannot be related to variations in the last term of equation 2 (the driving

force) as the redox potentials of the electron acceptors (Fe^{III} complex) are constant. The second (distance-dependent) term then emerges as the reason for differences in the value of k_4 from one mediator/HSO combination to the next. Conversely, heme-free HSO shows a higher outer sphere rate constant with $[\text{Fe}(\text{CN})_6]^{3-}$ ($k_4 = 1.0 \times 10^5 \text{ M}^{-1} \text{ s}^{-1}$) clearly indicating that the mediator charge plays a major role in determining the k_4 value. The calculated Michaelis constant $K_M = (k_2 + k_{-1})/k_1$ (Table 1) is consistent with the reported value ($9 \mu\text{M}$) from solution assays with natural electron acceptor cyt *c*.^[11b]

3. Conclusions

We have demonstrated the mediated catalytic voltammetry of holo and heme-free HSOs with both positively and negatively charged one-electron synthetic electron acceptors such as $[\text{Fe}(\text{dtne})]^{3+}$, FM^+ and $[\text{Fe}(\text{CN})_6]^{3-}$. We found that the mediator charge plays an important role in catalytic activity. The holo HSO enzyme shows enhanced catalytic activity with positively charged mediators. In contrast, heme-free HSO shows pronounced catalytic activity with a negatively charged mediator. These results show that positively charged $[\text{Fe}(\text{dtne})]^{3+}$ and FM^+ interact with the negatively charged cyt *b*₅ domain of HSO and negatively charged $[\text{Fe}(\text{CN})_6]^{3-}$ interacts with the positively charged Moco domain of HSO through electrostatic attraction which lead to effective electron transfer and enhanced electrocatalytic activity. A set of self-consistent rate constants was obtained for holo and heme-free HSO by simulating the experimental CVs measured at different sweep rates, mediators and substrate concentrations.

Experimental Section

Materials

Both holo and heme-free human sulfite oxidases (HSO) were purified in *E. coli* TP1000 as previously described.^[18] The iron complex 1,2-bis(1,4,7-triaza-1-cyclononyl)ethane iron(III) bromide

([Fe(dtne)]Br₃·3H₂O) was synthesized according to a published procedure.^[19] Ferrocene methanol (FM) was synthesized by NaBH₄ reduction of commercially available ferrocene carbaldehyde in MeOH, washing with water then extraction of the product into chloroform, which was pure by NMR.^[20] 5-(4'-Pyridinyl)-1,3,4-oxadiazole-2-thiol, potassium ferricyanide and sodium sulfite were purchased from Aldrich and were used as received. All other reagents used were of analytical grade purity and used without any further purification. Tris acetate buffer (50 mM) was used for all experiments at pH 8.0. All solutions were prepared with ultrapure water (resistivity 18.2 MΩ·cm) from a Millipore Milli-Q system.

Electrochemical Measurements and Electrode Cleaning

Cyclic voltammetry (CV) experiments were carried out with a BAS 100B/W electrochemical workstation. A three-electrode system was employed comprising a Au working electrode, a Pt wire counter, and an Ag/AgCl reference electrode (+196 mV vs NHE). Potentials are cited versus NHE. The gold working electrode was first cleaned according to a published protocol^[21] then modified with 5-(4'-pyridinyl)-1,3,4-oxadiazole-2-thiol as described.^[22] Experiments were carried on solutions that had been purged with Ar gas for 30 min.

The electro-active surface area of the Au electrode was determined from cyclic voltammetry of 1 mM ferrocene methanol^[20] in 0.1 M KCl solution at different sweep rates using the Randles-Sevcik equation (equation 3).^[13]

$$i_p = (2.69 \times 10^5) n^{3/2} A D_o^{1/2} C_o v^{1/2} \quad (3)$$

The diffusion coefficient (D_o) of ferrocene methanol is $6.7 \times 10^{-6} \text{ cm}^2 \text{ s}^{-1}$,^[23] i_p is the measured current maximum, n is the number of electrons (one in this case), C_o is concentration of analyte (mol cm^{-3}), and v is the sweep rate (V s^{-1}).

The variation of the catalytic peak current (i_{lim}) as a function of sulfite concentration was fit to Michaelis–Menten kinetics (equation 4) yielding $K_{M,app}$ (the apparent Michaelis constant) and i_{max} (the effective electrochemical turnover number, $i_{max} = nFA[HSO]$).^[24]

$$i_{lim} = \frac{i_{max}[SO_3^{2-}]}{K_{M,app} + [SO_3^{2-}]} \quad (4)$$

Enzyme Electrode Preparation

A 3 μ L droplet of either holo HSO (50 μ M) or heme-free HSO (50 μ M) in 50 mM Tris buffer (pH 8.0) was pipetted onto the conducting surface of an inverted, freshly prepared Au/Hpyt working electrode and this was allowed to dry a film at 4°C. To prevent protein loss, the electrode surface was carefully covered with a perm-selective dialysis membrane (Molecular weight cut off 3500 Da), presoaked in water. The dialysis membrane was pressed onto the electrode with a Teflon cap and fastened to the electrode with a rubber O-ring to prevent leakage of the internal membrane solution. The resulting modified electrode was stored at 4°C in 50 mM Tris buffer (pH 8.0) when not in use. The HSO enzyme was confined to a thin layer beneath the membrane while substrate and mediators were able to diffuse across the dialysis membrane.

Electrochemical Simulation

DigiSim (version 3.03b) was employed to simulate the experimental cyclic voltammograms.^[25] The experimental parameters restrained in each case were the working electrode surface area ($A = 0.055 \text{ cm}^2$) and the double-layer capacitance (12 μ F). Semi-infinite diffusion was assumed and all pre-equilibration reactions were enabled. The apparent redox potential of mediators was determined from control voltammetry experiments in the absence of enzyme or substrate. The diffusion coefficients of mediators were also obtained in the presence of a dialysis membrane covering the electrode by simulation of the cyclic voltammetry at different sweep rates in the absence of substrate and enzyme to

give value of $5 \times 10^{-7} \text{ cm}^2 \text{ s}^{-1}$. This value is slightly higher than the reported value for FM ($6.7 \times 10^{-6} \text{ cm}^2 \text{ s}^{-1}$)^[23] and $\text{K}_3[\text{Fe}(\text{CN})_6]$ ($7.6 \times 10^{-6} \text{ cm}^2 \text{ s}^{-1}$)^[26] which is a consequence of mass transport limitations by the dialysis membrane.^[14b] The diffusion coefficients for HSO and sulfite were taken to be $2 \times 10^{-7} \text{ cm}^2 \text{ s}^{-1}$ and $5 \times 10^{-6} \text{ cm}^2 \text{ s}^{-1}$.^[14b] These values were kept constant for all experiments. The heterogeneous rate constant (k_0) was determined from simulating the sweep rate dependence of the anodic peak to cathodic peak separation of mediators (in the absence of HSO) and then held constant thereafter. The enzyme dependent parameters (k_1/k_{-1} , k_2/k_{-2} , k_3/k_{-3}) were determined for one set of experiments carried out with different sulfite concentrations and sweep rates and then kept the same for all experiments, regardless of mediator. The only rate constants that were allowed to refine were those for the outer sphere electron transfer reactions between each mediator and HSO (k_4 , $k_{4'}$, k_{-4} and $k_{-4'}$ in Scheme 1). The oxidation of either the Mo^{IV} or Mo^{V} forms of HSO was assumed to proceed at the same rate thus $k_4 = k_{4'}$ and $k_{-4} = k_{-4'}$.^[27]

Acknowledgements

PVB acknowledges financial support from the Australian Research Council (DP150103345).

Keywords

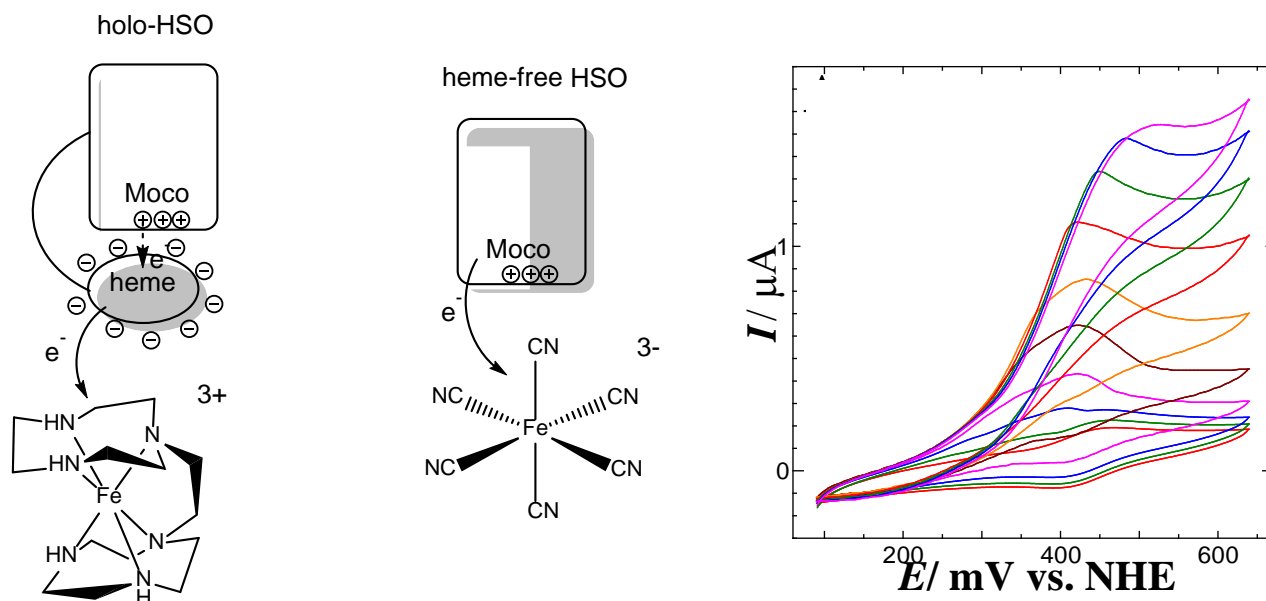
Cyclic voltammetry, enzymes, electron transfer

5. References

- [1] a) C. Kisker, H. Schindelin, A. Pacheco, W. A. Wehbi, R. M. Garrett, K. V. Rajagopalan, J. H. Enemark, D. C. Rees, *Cell* **1997**, *91*, 973-983; b) R. Hille, J. Hall, P. Basu, *Chem. Rev.* **2014**, *114*, 3963-4038.
- [2] B. C. Schwahn, F. J. Van Spronsen, A. A. Belaidi, S. Bowhay, J. Christodoulou, T. G. Derks, J. B. Hennermann, E. Jameson, K. König, T. L. McGregor, E. Font-Montgomery, J. A. Santamaria-Araujo, S. Santra, M. Vaidya, A. Vierzig, E. Wassmer, I. Weis, F. Y. Wong, A. Veldman, G. Schwarz, *Lancet* **2015**, *386*, 1955-1963.
- [3] M. J. Rudolph, J. L. Johnson, K. V. Rajagopalan, C. Kisker, *Acta Crystallogr. Sect. D. Biol. Crystallogr.* **2003**, *59*, 1183-1191.
- [4] M. S. Brody, R. Hille, *Biochemistry* **1999**, *38*, 6668-6677.
- [5] a) S. J. Elliott, A. E. McElhaney, C. Feng, J. H. Enemark, F. A. Armstrong, *J. Am. Chem. Soc.* **2002**, *124*, 11612-11613; b) E. E. Ferapontova, T. Ruzgas, L. Gorton, *Anal. Chem.* **2003**, *75*, 4841-4850; c) E. E. Ferapontova, A. Christenson, A. Hellmark, T. Ruzgas, *Bioelectrochemistry* **2004**, *63*, 49-53; d) S. Frasca, A. Molero Milan, A. Guet, C. Goebel, F. Pérez-Caballero, K. Stiba, S. Leimkühler, A. Fischer, U. Wollenberger, *Electrochim. Acta* **2013**, *110*, 172-180; e) T. Zeng, S. Leimkühler, J. Koetz, U. Wollenberger, *ACS Appl. Mat. Inter.* **2015**, *7*, 21487-21494; f) S. Frasca, O. Rojas, J. Salewski, B. Neumann, K. Stiba, I. M. Weidinger, B. Tiersch, S. Leimkuehler, J. Koetz, U. Wollenberger, *Bioelectrochemistry* **2012**, *87*, 33-41; g) T. Zeng, S. Frasca, J. Rumschöttel, J. Koetz, S. Leimkühler, U. Wollenberger, *Electroanalysis* **2016**, *28*, 2303-2310.
- [6] a) H. L. Wilson, K. V. Rajagopalan, *J. Biol. Chem.* **2004**, *279*, 15105-15113; b) M. Sezer, R. Spricigo, T. Utesch, D. Millo, S. Leimkuehler, M. A. Mroginski, U. Wollenberger, P. Hildebrandt, I. M. Weidinger, *Phys. Chem. Chem. Phys.* **2010**, *12*, 7894-7903; c) R. Spricigo, S. Leimkühler, L. Gorton, F. W. Scheller, U. Wollenberger, *Eur. J. Inorg. Chem.* **2015**, *2015*, 3526-3531; d) U. Wollenberger, R. Spricigo, S. Leimkuehler, K. Schroeder, *Adv. Biochem. Eng./Biotechnol.* **2008**, *109*, 19-64.
- [7] a) T. Aono, Y. Sakamoto, M. Miura, F. Takeuchi, H. Hori, M. Tsubaki, *J. Biomed. Sci.* **2010**, *17*, 1-15; b) S. Bagby, P. D. Barker, L. H. Guo, H. A. O. Hill, *Biochemistry* **1990**, *29*, 3213-3219; c) M. Rivera, M. A. Wells, F. A. Walker, *Biochemistry* **1994**, *33*, 2161-2170.
- [8] J. L. Johnson, K. V. Rajagopalan, *J. Biol. Chem.* **1977**, *252*, 2017-2025.
- [9] P. Kalimuthu, A. A. Belaidi, G. Schwarz, P. V. Bernhardt, *Electrochim. Acta* **2016**, *199*, 280-289.
- [10] K. Johnson-Winters, A. R. Nordstrom, S. Emesh, A. V. Astashkin, A. Rajapakshe, R. E. Berry, G. Tollin, J. H. Enemark, *Biochemistry* **2010**, *49*, 1290-1296.
- [11] a) A. Pacheco, J. T. Hazzard, G. Tollin, J. H. Enemark, *J. Biol. Inorg. Chem.* **1999**, *4*, 390-401; b) A. Rajapakshe, K. T. Meyers, R. E. Berry, G. Tollin, J. H. Enemark, *J. Biol. Inorg. Chem.* **2012**, *17*, 345-352; c) K. Johnson-Winters, A. C. Davis, A. R. Arnold, R. E. Berry, G. Tollin, J. H. Enemark, *J. Biol. Inorg. Chem.* **2013**, *18*, 645-653.
- [12] P. Zuo, T. Albrecht, P. D. Barker, D. H. Murgida, P. Hildebrandt, *Phys. Chem. Chem. Phys.* **2009**, *11*, 7430-7436.
- [13] A. J. Bard, L. R. Faulkner, *Electrochemical Methods: Fundamentals and Applications*, **2001**.
- [14] a) P. Kalimuthu, M. D. Heath, J. M. Santini, U. Kappler, P. V. Bernhardt, *Biochim. Biophys. Acta - Bioenerg.* **2014**, *1837*, 112-120; b) P. Kalimuthu, U. Kappler, P. V. Bernhardt, *J. Phys. Chem. B* **2014**, *118*, 7091-7099; c) P. Kalimuthu, J. Heider, D. Knack, P. V. Bernhardt, *J. Phys. Chem. B* **2015**, *119*, 3456-3463.

- [15] a) P. Kalimuthu, J. Tkac, U. Kappler, J. J. Davis, P. V. Bernhardt, *Anal. Chem.* **2010**, *82*, 7374-7379; b) P. Kalimuthu, S. Leimkühler, P. V. Bernhardt, *J. Phys. Chem. B* **2011**, *115*, 2655-2662.
- [16] a) K.-I. Chen, A. G. McEwan, P. V. Bernhardt, *J. Biol. Inorg. Chem.* **2009**, *14*, 409-419; b) K.-I. Chen, A. G. McEwan, P. V. Bernhardt, *J. Biol. Inorg. Chem.* **2011**, *16*, 227-234.
- [17] C. C. Page, C. C. Moser, X. Chen, P. L. Dutton, *Nature* **1999**, *402*, 47-52.
- [18] A. A. Belaidi, G. Schwarz, *Biochem. J.* **2013**, *450*, 149-157.
- [19] K. Wieghardt, I. Tolksdorf, W. Herrmann, *Inorg. Chem.* **1985**, *24*, 1230-1235.
- [20] G. D. Broadhead, J. M. Osgerby, P. L. Pauson, *J. Chem. Soc.* **1958**, 650-656.
- [21] J. Tkac, J. J. Davis, *J. Electroanal. Chem.* **2008**, *621*, 117-120.
- [22] T. d. F. Paulo, M. A. S. da Silva, S. d. O. Pinheiro, E. Meyer, L. S. Pinheiro, J. A. Freire, A. A. Tanaka, P. de Lima Neto, I. d. S. Moreira, I. C. N. Diogenes, *J. Braz. Chem. Soc.* **2008**, *19*, 711-719.
- [23] N. Anicet, C. Bourdillon, J. Moiroux, J.-M. Saveant, *J. Phys. Chem. B* **1998**, *102*, 9844-9849.
- [24] M. Situmorang, D. B. Hibbert, J. J. Gooding, D. Barnett, *Analyst* **1999**, *124*, 1775-1779.
- [25] M. Rudolf, S. W. Feldberg, *DigiSim version 3.03b. Bioanalytical System, West Lafayette* **2004**.
- [26] Y. S. Grewal, M. J. A. Shiddiky, S. A. Gray, K. M. Weigel, G. A. Cangelosi, M. Trau, *Chem. Commun.* **2013**, *49*, 1551-1553.
- [27] J. T. Spence, C. A. Kipke, J. H. Enemark, R. A. Sunde, *Inorg. Chem.* **1991**, *30*, 3011-3015.

Table of Contents



Charge is important in determining the rates of intermolecular electron transfer between human sulfite oxidase (HSO) and various synthetic electron transfer mediators. Holo-HSO prefers positively charged mediators akin to its natural electron partner cytochrome *c* while heme-free HSO is better suited to negatively charged electron acceptors that mimic its missing heme cofactor.